Robotica (2014) volume 32, pp. 1081–1100. © Cambridge University Press 2014
doi:10.1017/S0263574713001264

Clinical experimental research on adaptive robot-aided therapy control methods for upper-limb rehabilitation

Guozheng Xu†* , Aiguo Song‡, Lizheng Pan‡, Xiang Gao†, Zhiwei Liang†, Jinfei Li§ and Baoguo Xu‡

†*College of Automation, Nanjing University of Posts and Telecommunications, Nanjing 210046, P. R. China*
‡*School of Instrument Science and Engineering, Southeast University, Nanjing 210096, P. R. China*
§*Department of Rehabilitation Medicine of Nanjing Tongren Hospital, Nanjing 211102, P. R. China*

(Accepted December 11, 2013. First published online: January 15, 2014)

SUMMARY
This study presents novel robotic therapy control algorithms for upper-limb rehabilitation, using newly developed passive and progressive resistance therapy modes. A fuzzy-logic based proportional-integral-derivative (PID) position control strategy, integrating a patient's biomechanical feedback into the control loop, is proposed for passive movements. This allows the robot to smoothly stretch the impaired limb through increasingly rigorous training trajectories. A fuzzy adaptive impedance force controller is addressed in the progressive resistance muscle strength training and the adaptive resistive force is generated according to the impaired limb's muscle strength recovery level, characterized by the online estimated impaired limb's bio-damping and bio-stiffness. The proposed methods are verified with a custom constructed therapeutic robot system featuring a Barrett WAM^{TM} compliant manipulator. Twenty-four recruited stroke subjects were randomly allocated in experimental and control groups and enrolled in a 20-week rehabilitation training program. Preliminary results show that the proposed therapy control strategies can not only improve the impaired limb's joint range of motion but also enhance its muscle strength.

KEYWORDS: Rehabilitation robot; Clinical experiment; Fuzzy logic; Position control; Impedance control.

1. Introduction

In recent years, there has been an increasing interest in using robotic devices to help provide rehabilitation therapy for stroke patients.[1] Therapeutic controller design is one of the major difficulties for realizing robot-aided neurorehabilitation. Research on human biomechanics and manual physical therapy practice suggests that the robotic therapy control strategies should vary with the recovery state of a patient's physical condition.

In the early stage, when patients have extremity motor dysfunction, smooth stretching exercises can help prevent stiffening of soft tissue and reduce spasticity.[2] For robot-aided therapy in this stage, the position controller must, stably and smoothly, stretch the impaired limb along predefined training trajectories and achieve normative joint movement patterns. Several categories of position controllers for passive training have been developed in the last few years.[3,4] Although they verify the position tracking advantages, few of the studies apply the controllers in clinical trials. It is well known that the change in muscle tone for healthy and hemiparetic subjects undergoing passive stretching should be characterized differently: the former by uniform rigidity and the latter by cogwheel rigidity. In addition, a common problem in most of the existing position controllers is that they are implemented

* Corresponding author. E-mail: xgznjupt@gmail.com

https://doi.org/10.1017/S0263574713001264 Published online by Cambridge University Press

in an open-loop manner while not incorporating the stroke patient into the control loop. Integrating the patient into the system and achieving cooperative rehabilitation will make the training system more compliant, safe and acceptable.[5]

In the case when the impaired limb has the ability to move against a certain resistive force freely, progressive resistance muscle strength training with a force-based therapy control algorithm should be supplied. Impedance control, one of the most effective force control methods, is often adopted in robot-aided rehabilitation training. Frisoli *et al.*[6] presented an impedance-based force feedback exoskeleton (L-EXOS) and verified the training system efficacy with virtual reaching exercises for eight post-stroke subjects. Veneman *et al.*[7] confirmed the feasibility of unhindered walking and achieving a normal gait pattern on a bidirectional impedance-controlled gait rehabilitation device, LOPES. However, the potential issue for the aforementioned impedance-based therapy control strategies is that the mechanical impedance between the robot and the impaired limb cannot be real time regulated. It is obvious that a robot-aided training system that can provide adaptive functional training, corresponding to the patient's progress, will be more effective. This is especially true in progressive resistance training where the exerted resistive force that is too small for the subject will be perceived as boring, while the force that is too large will overstress the subject. Only an adaptive resistive force that adjusts in real time to consistently challenge the patient will induce maximal engagement and optimal physical participation. Kiguchi *et al.*[8,9] proposed adaptive impedance controllers for an upper limb rehabilitation exoskeleton where the desired impedance parameters were regulated according to the human muscle EMG signal changes. In our previous studies,[10,11] adaptive impedance force controllers were employed to generate an adaptive force corresponding to the arm muscle strength changes. Other adaptive impedance force controllers were also developed in recent emerging rehabilitation devices.[12,13] Although shown to be effective to some extent, most of these impedance force controllers are mainly focused on providing active-assisted exercises. Few attempts are made in progressive resistance muscle strength training. In addition, clinical trials need to be carried out with stroke subjects to gauge the effectiveness of the existing force controllers.

In this paper, clinical experiments were performed with necessary improvements to the adaptive robot-aided therapy control methods presented in our previous work.[10] The study's objectives were to (i) evaluate the clinical utility of the current therapeutic robotic system with improved therapy control methods, and (ii) explore the efficacy of this new type of robot-aided therapy as compared to standard physiotherapy treatment for post-stroke subjects. The remainder of this paper is organized as follows: Section 2 presents the recruited participants, experimental setup, clinical training protocols, and improved therapy control methods. Section 3 details the results of the proposed therapy control algorithm for the passive position control, progressive resistive force regulation, and therapy outcome comparison. Some discussion and conclusions are presented in Sections 4 and 5, respectively.

2. Methods

2.1. Subjects

Stroke subjects with upper extremity motor impairments and activity limitations, aged 50 years and over, were recruited as representative of hemiparesis participants. Participants were excluded from the study if they had epilepsy, severe neurological disorder, or senile dementia.[14] If the individuals met the inclusion criteria and gave informed consent, they were then assessed by an occupational therapist. Forty-five participants, from Zhongda Hospital affiliated Southeast University (24) and Nanjing Tongren Hospital (21), were recruited. A physiotherapist, not affiliated with this study, randomized the recruited participants into one of two groups: experimental (robot-aided therapy) group and control group (conventional therapist therapy), using a random number table. The participants' demographic characteristics are shown in Table I.

2.2. Experimental setup

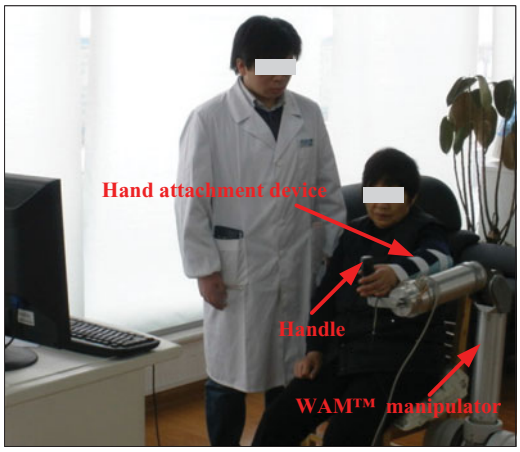
The prototype therapeutic robotic system for upper-limb rehabilitation used in the trials, shown in Fig. 1, consists of a Barrett WAM^{TM} manipulator, a three-dimensional (3D) force sensor, a hand attachment device with a handle, and an external PC offered by Barrett Technology.[15] The standard WAM is a four-degree-of-freedom highly dexterous, naturally back-drivable manipulator. In order to record the force between the impaired limb and the WAM end-effector, an improved 3D force sensor[16]

https://doi.org/10.1017/S0263574713001264 Published online by Cambridge University Press

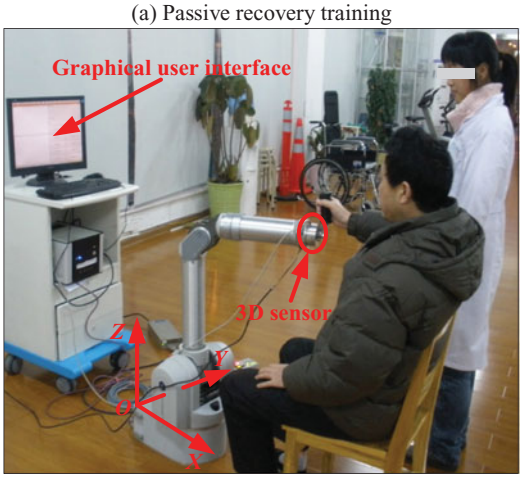
Table I. Demographic characteristics of recruited stroke subjects.

Subject group	*N*	Mean age (years)	Gender (M/F)	Mean stroke time (months)	Stroke degree (S/M/M)
Robot group	23	53.6	15/8	12.6	5/14/4
Control group	22	56.9	12/10	14.3	7/10/5

Note: Gender: M = male; F = female; stroke degree: S = severe; M = moderate; M = mild.



(a) Passive recovery training



(b) Active or progressive resistance training

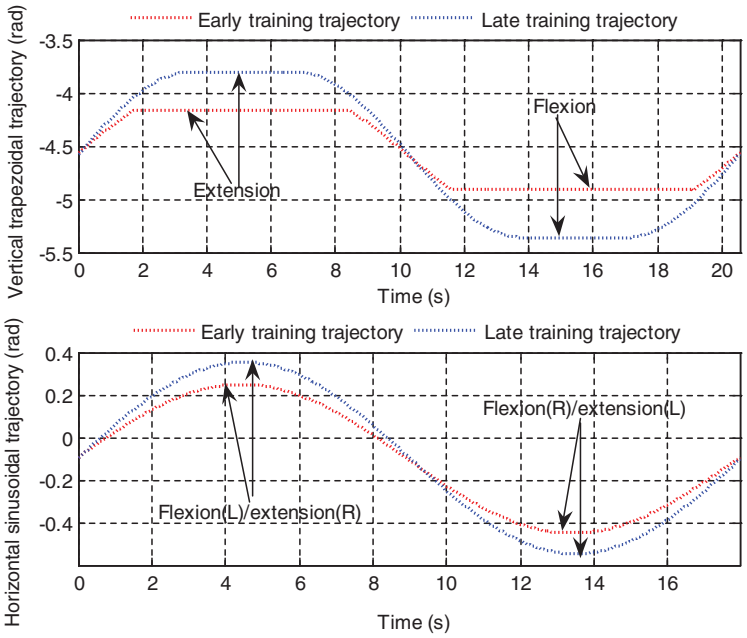
Fig. 1. (Colour online) The therapeutic robotic system prototype with Barrett WAM^{TM} and training modes: (a) passive recovery training; (b) active or progressive resistance training.

was designed and attached to the end-effector. The hand attachment device allows the forearm of the stroke subject to be well supported as they perform the passive exercises (Fig. 1(a)). The external PC, with the Ubuntu Linux operating system and the real-time module, Xenomai, was responsible for running the control loop and providing high-level command of the WAM rehabilitation system. In the active or progressive resistance training (Fig. 1(b)), a graphical user interface is used that displays both the planed and actual trajectories. All real-time communication between the external PC and motor Pucks^{TM} (motor controllers) may be via an internal high-speed controller area network (CAN) bus, a high-speed Ethernet cable, or wireless-Ethernet. High-speed CAN bus communication was used in this research.

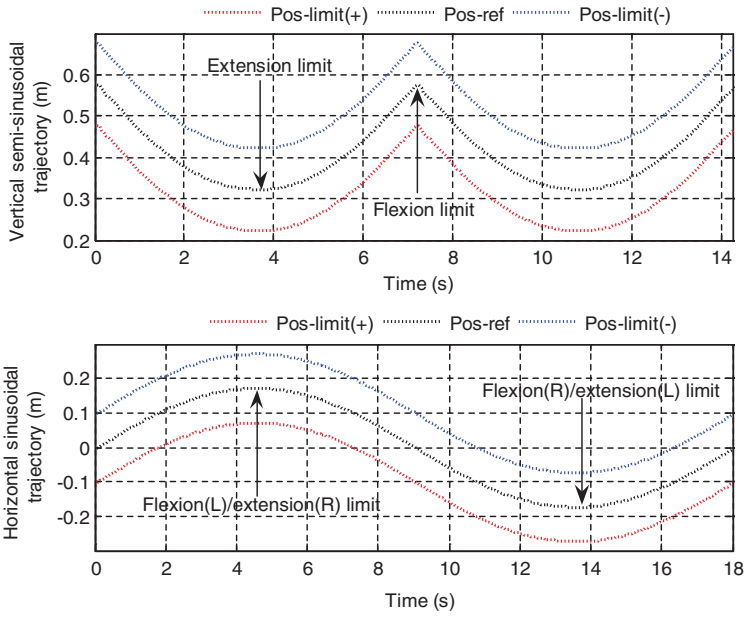
2.3. Training protocol

2.3.1. Experimental group. Individuals randomized to the robot experimental group received WAM-aided upper limb rehabilitation therapy in passive and progressive resistance training modes. For the

https://doi.org/10.1017/S0263574713001264 Published online by Cambridge University Press



(a) Example of an increasing training trajectory in passive training



(b) Progressive resistance training trajectory

Fig. 2. (Colour online) Description of representative training trajectories: (a) example of an increasing training trajectory in passive training; (b) progressive resistance training trajectory.

passive movement, trapezoidal and sinusoidal trajectories (Fig. 2(a)) were planned in WAM joint space, and both were used for vertical elbow joint and horizontal shoulder joint flexion/extension exercises. As the impaired limb's joint range of motion (ROM) recovers, small angle increments were added. In the early stage of passive training, the trapezoidal trajectory was used to perform intermittent exercise where the impaired limb would be held at the extreme position for a period of time. After a specified number of training cycles, the sinusoidal trajectory was used to implement continuous training. After the passive stretching treatment, active recovery movements were performed where no controllers were implemented except for the full gravity compensation for the WAM. The aim of the active recovery movements was to improve the impaired limb's joint coordinate ability and make

https://doi.org/10.1017/S0263574713001264 Published online by Cambridge University Press

preparations for the subsequent progressive résistance training. Clinicians used their professional judgments to tailor progressive resistance training. Once the patient had the ability to move her/his body freely against gravity, the progressive resistance training was carried out. The patient was asked to move the WAM along semi-sinusoidal and sinusoidal trajectories (Fig. 2(b)) planned in the WAM Cartesian space for vertical elbow and horizontal shoulder flexion/extension, respectively.

A teach and replay technique was introduced in both therapy modes to generate the desired trajectory for the impaired limb. The unimpaired limb's normative movement was prerecorded and then re-optimized using linear interpolation with parabolic blends algorithm.

2.3.2. Control group. Individuals randomized to the control group received conventional therapist therapy. Assorted techniques and progressive programs for upper extremity retaining were used by treating therapists.

For both groups, the training program consisted of two-hour training session a day six times a week over a 20-week duration, including, on average, six-week passive, six-week active, and eight-week resistive training exercises.

2.3.3. Outcome measure. The WAM-aided rehabilitation training system was used as the main therapy outcome test platform, and robotic measured parameters were objectively selected as quantitative evaluation indices. A research technician from Southeast University collected the biomechanical and progress data from the WAM-aided therapeutic system at the start and end of the treatment for both groups. To ensure there was no bias in comparing the two groups, patients allocated to the experimental group were allowed to become familiar with the robot-aided training environment before therapy outcome evaluation procedure was carried out. This procedure included the following outcome measure parameters:

Passive range of motion (PROM): Extreme joint range of motion with the assistance of WAM or therapist for elbow vertical and shoulder horizontal flexion/extension was assessed.

Maximum resistive force (MRF): An increasing resistive force generated from the WAM control program was imposed on the impaired limb to keep the subject's upper arm vertical and forearm horizontal. The maximum force that could be overcome by the subject during movements was recorded.

2.4. Controller design

2.4.1. Position controller

A. Position controller design for passive movement

Figure 3 gives the block diagram of the proposed fuzzy-logic proportional-integral-derivative (PID) position controller, which is composed of the fuzzy PID regulator, real-time biomechanical reflection data from the stroke subject, and software-based gravity compensation. The regulator has separate fuzzy logic for the proportional (P), integral (I), and derivative (D) components.θ_{e} and θ_{ec}, joint position error and error change respectively, were chosen as input variables. Controller gain increments ΔK_P, ΔK_I, ΔK_D are set as the corresponding outputs. In the fuzzification process, the input and output of the fuzzy regulator are scaled and mapped to five triangle-shaped or trapezoidal membership functions, namely, negative big (NB), negative small (NS), zero (ZE), positive small (PS), and positive big (PB). The fuzzy inference rules and membership functions (MFs) for the input and output variables are shown in Table II and Fig. 4, respectively. Generally, if the joint position tracking error θ_{e} and error change θ_{ec} are positive (PB or PS), implying the trajectory tracking performance partly resulting from the patient's motion chattering disturbance would be worse, then proper increments (PB, PS, or ZE) should be added to ΔK_P, ΔK_I, and ΔK_D. On the contrary, if θ_{e} and θ_{ec} are negative (NB or NS), then the controller has sufficient control capability to drive the impaired limb, progressively achieving a normative joint movement pattern, and a proper decrement (NB, NS, or ZE) might be supplied. Further, if θ_{e} and θ_{ec} do not change substantially (ZE), no increments or decrements are needed to add to ΔK_P,ΔK_I, and ΔK_D. If θ_{e} and θ_{ec} had opposite changes, then proper increments (negative error change) or decrements (positive error change) were added to the three gains. The outputs (ΔK_P,ΔK_I,ΔK_D) from the fuzzy regulator are linearly combined with a traditional PID

https://doi.org/10.1017/S0263574713001264 Published online by Cambridge University Press

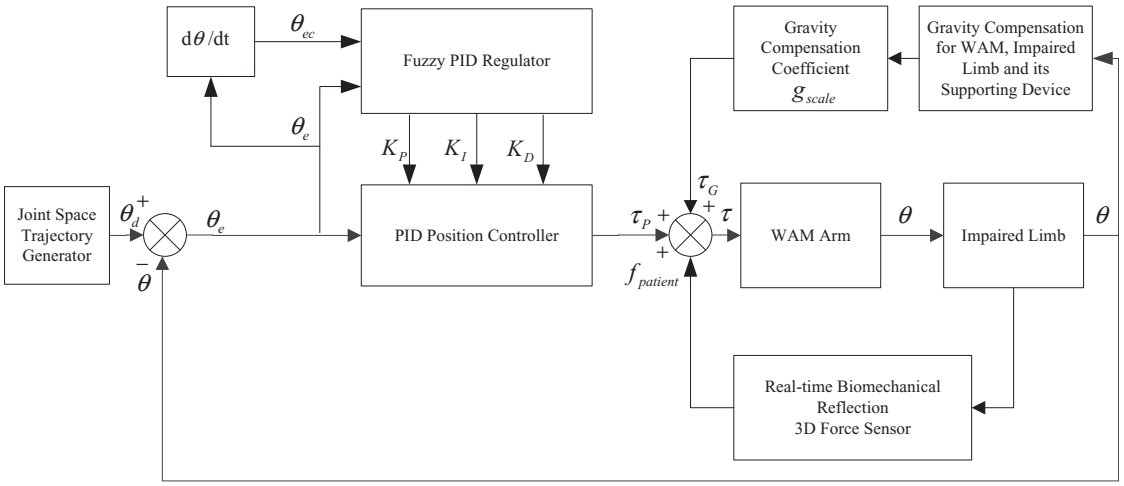


Fig. 3. Block diagram of fuzzy-based PID position controller.

Table II. Fuzzy control rules for the gain increments ΔK_P,ΔK_I, and ΔK_D.

		θ_{ec}				
$\Delta K_P/\Delta K_I/\Delta K_D$		NB	NS	ZE	PS	PB
θ_e	NB	NB/NB/NB	NS/NS/NS	NS/ZE/NS	NS/NS/ZE	PS/PS/PS
	NS	NS/NS/NS	NS/ZE/ZE	ZE/ZE/NS	ZE/PS/ZE	PS/PS/PS
	ZE	NS/ZE/NS	ZE/ZE/ZE	ZE/ZE/ZE	ZE/PS/ZE	PS/PS/PB
	PS	PS/PS/PS	ZE/PS/PS	ZE/ZE/PS	PS/PS/PS	PS/PS/PB
	PB	PB/PS/PB	PS/PS/PS	PS/ZE/PB	PB/PS/PB	PS/PS/PS

controller (K_P,K_I,K_D):

$$\tau_P = (K_P + \Delta K_P)(\theta_d - \theta) + (K_D + \Delta K_D)\frac{\mathrm{d}(\theta_d - \theta)}{\mathrm{d}t} + \int (K_I + \Delta K_I)(\theta_d - \theta)\mathrm{d}t, \quad (1)$$

where θ_d and θ are the desired and actual joint positions, respectively. τ_P is the controller output torque.

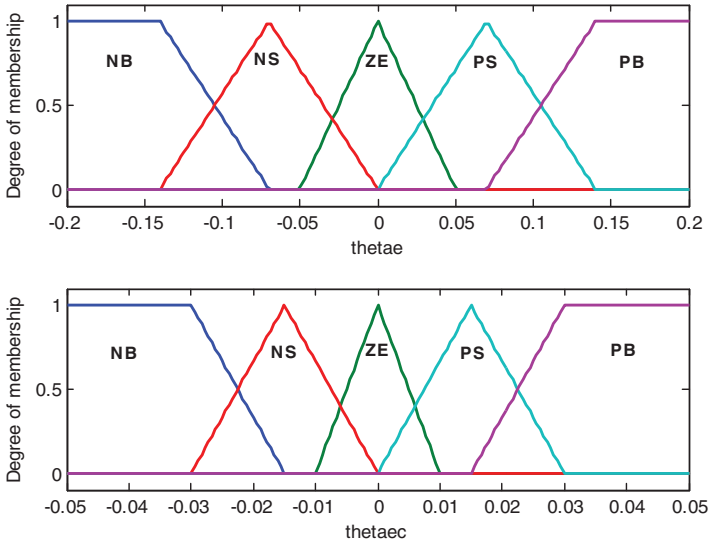
Differing from the healthy subject verification in our previous work,[10] the real-time biomechanical reflection module is used to achieve close-loop motion control by incorporating the patient's motor chatter disturbance f_{patient} into the control loop. It is expected that the patient would still be stretched stably and smoothly even in the presence of the patient's chatter vibration disturbance.

Another important consideration for the WAM-aided physiotherapy is gravity compensation for the WAM and its attachment devices, which are significant barriers to exercise. A software-based gravity compensation technique is adopted in this research, which offers the flexibility to easily modulate the amount of compensation provided in different recovery movements. A gravity compensation coefficient g_{scale} is set and Eq. (1) can now be written as

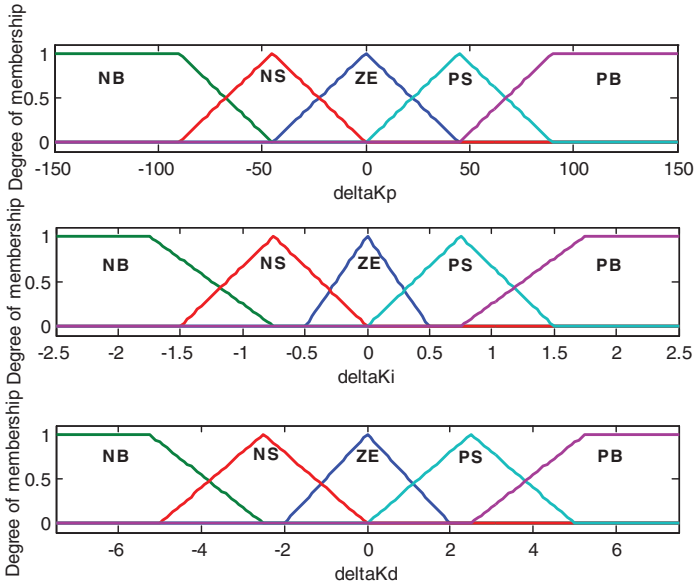
$$\tau = (K_P + \Delta K_P)(\theta_d - \theta) + (K_D + \Delta K_D)\frac{\mathrm{d}(\theta_d - \theta)}{\mathrm{d}t} + \int (K_I + \Delta K_I)(\theta_d - \theta)\mathrm{d}t + \tau_{f_{\text{patient}}} + M \cdot g_{\text{scale}} \cdot g, \quad (2)$$

where M includes the mass vector of the WAM link, the hand attachment device and the patient's forearm. $\tau_{f_{\text{patient}}}$ is the torque caused by the patient's chatter disturbance f_{patient}, g is the gravity acceleration vector in the link frames, and g_{scale} is the gravity compensation scales.

https://doi.org/10.1017/S0263574713001264 Published online by Cambridge University Press



(a) Membership functions for input variables



(b) Membership functions for output variables

Fig. 4. (Colour online) Description of membership functions for input and output variables in fuzzy position controller: (a) membership functions for input variables; (b) membership functions for output variables.

B. Analysis of stability and smoothness performance

Since unpredictable chatter vibration disturbance from the patient is very likely in the WAM-aided rehabilitation process, analysis of the stability and smoothness of the proposed fuzzy-based PID position controller must be performed. Passive control theory, a stability analysis method often used in bilateral control of teleoperators,[17] is introduced here to analyze the rehabilitation robot stability and smoothness when interacting with patient. The main idea of this analytical method is that an equivalent two-port circuit of the rehabilitation robot and impaired limb is built based on the equivalent rule between an electrical system and a mechanical system. By drawing equivalences, such as current with velocity and voltage with force, constructing the system's entire dynamic model is not needed. The system is considered as stable if and only if the equivalent two-port circuit is passive, that is, the circuit may dissipate energy but cannot increase the system's total energy. Detailed analysis and the full proof may be referred to in our recent work.[18] According to the analysis, the bounds of the

https://doi.org/10.1017/S0263574713001264 Published online by Cambridge University Press

controller gains P, I, and D, adjusted by fuzzy regulator, may be determined to ensure the system's stability and smoothness.

2.4.2. Force controller

A. Estimation of the patient's biomechanical state

As mentioned in refs. [19] and [20], the human arm's bio-impedance parameters, bio-damping and bio-stiffness, can reflect the arm's muscle power changes with high sensitivity. Based on our previous work in ref. [10], the impaired limb's bio-impedance characteristic is modeled as the following linear time-variant system:

$$f_e(t) = b_e(t)\delta\dot{x}(t) + k_e(t)\delta x(t), \tag{3}$$

where f_e denotes the interaction force between the robot and the impaired limb, $\delta x = x - x_e$ is the displacement between the actual and equilibrium positions of the impaired limb, $\delta\dot{x}$ is the velocity vector, and b_e and k_e denote the impaired limb's bio-damping/stiffness.

Using the bilinear transformation in ref. [21], Eq. (3) is reorganized in the discrete-time domain as

$$f_e(z) = \left[b_e(z)\left(\frac{2}{T}\right)\left(\frac{1-z^{-1}}{1+z^{-1}}\right) + k_e(z)\right]\delta x(z), \tag{4}$$

where T is the sampling period and z^{-1} is one shift step in the time domain. Using Eq. (4), the continuous linear model is discretized to provide a model for linear estimation:

$$f_e(k) + f_e(k-1) = a_1(k)\delta x(k) + a_2(k)\delta x(k-1), \tag{5}$$

where

$$a_1(k) = b_e(k)\left(\frac{2}{T}\right) + k_e(k),\ a_2(k) = k_e(k) - b_e(k)\left(\frac{2}{T}\right).$$

Furthermore, Eq. (5) is represented as a regression vector, which is as follows:

$$\begin{aligned} &y[k] = h^{\mathrm{T}}[k]\theta[k], \quad \theta[k] = [a_1(k), a_2(k)]^{\mathrm{T}}, \\ &h[k] = [\delta x(k), \delta x(k-1)]^{\mathrm{T}}, \quad y[k] = f_e(k) + f_e(k-1), \end{aligned} \tag{6}$$

where $\theta[k]$ is the estimated parameter vector, and $h[k]$ and $y[k]$ represent the input and output regression vectors, respectively.

According to the regressive least square method with forgetting factor (FRLS), we have

$$\theta[k] = \theta[k-1] + \frac{P[k-1]h[k]\left(y[k] - h^{\mathrm{T}}[k]\theta[k-1]\right)}{\lambda + h^{\mathrm{T}}[k]P[k-1]h[k]}, \tag{7}$$

where λ is the constant forgetting factor, which influences the weight given to the earlier data relative to the newly acquired data. The covariance matrix $P[k]$ can be calculated as follows:

$$P[k] = \frac{1}{\lambda}\left(P[k-1] - \frac{P[k-1]h[k]h^{\mathrm{T}}[k]P[k-1]}{\lambda + h^{\mathrm{T}}[k]P[k-1]h[k]}\right). \tag{8}$$

In ref. [21], the estimated results using the above FRLS method are still not satisfactory, especially for the damping coefficient, although the given environment parameters, stiffness and damping, are constant. In robot-aided clinical rehabilitation, the impaired limb's dynamics vary randomly and its bio-impedance parameters are time-variant throughout the rehabilitation process. It is suggested that the estimation of the impaired limb's bio-impedance parameters using RLS with an adaptive forgetting factor (AFRLS) is superior to the one with a fixed forgetting factor. The forgetting factor

https://doi.org/10.1017/S0263574713001264 Published online by Cambridge University Press

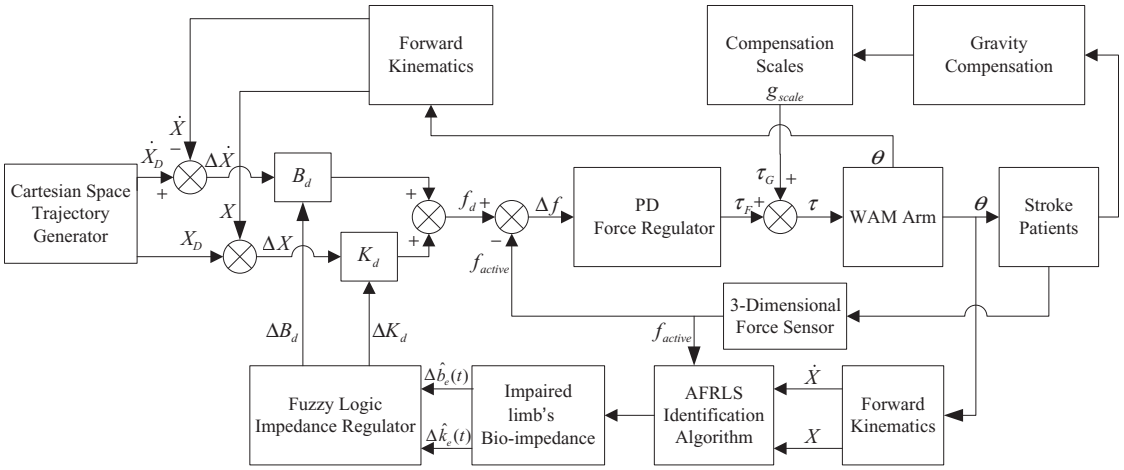


Fig. 5. Block diagram of fuzzy-based impedance force controller.

is adapted as

$$\lambda[k] = 1 - \left[1 - \frac{h^T(k-l-1)P[k-1]h(k-l-1)}{1+h^T(k-l-1)P[k-1]h(k-l-1)}\right] \times \left[\frac{\left(y[k]-h^{\mathrm{T}}[k]\theta[k-1]\right)^2}{R}\right], \quad (9)$$

where l and R are the forgetting step and the parameter respectively. In addition, the maximum and minimum forgetting factors, $\lambda_{\max}$ and $\lambda_{\min}$ respectively, are set for preventing unfortunate disturbances. After the vector θ is estimated, the impaired limb's bio-damping $\hat{b}_e$ and bio-stiffness $\hat{k}_e$ are obtained from Eq. (5):

$$\hat{b}_e(k) = T\left(\frac{a_1(k)-a_2(k)}{4}\right) \hat{k}_e(k) = \frac{a_1(k)+a_2(k)}{2}. \quad (10)$$

B. Fuzzy adaptive impedance force controller

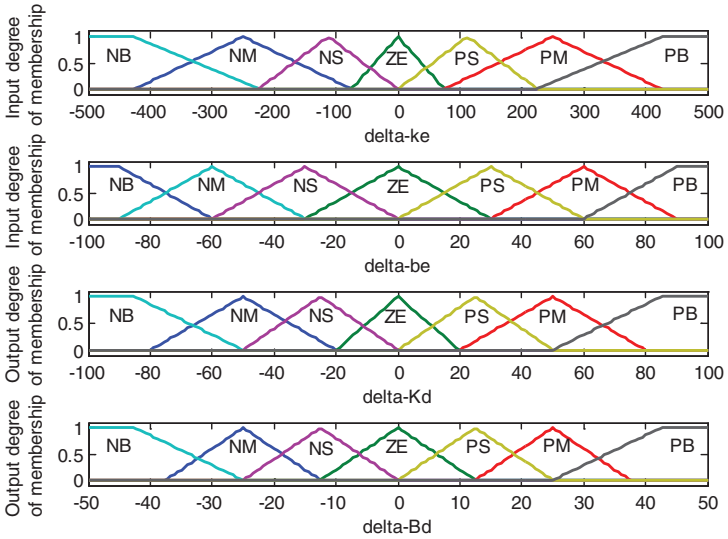
Based on our previous work in ref. [10], the impedance property between the WAM end-effector and the impaired limb in the Cartesian space is summarized as

$$B_d(\dot{X}_d - \dot{X}) + K_d(X_d - X) = F_d, \quad (11)$$

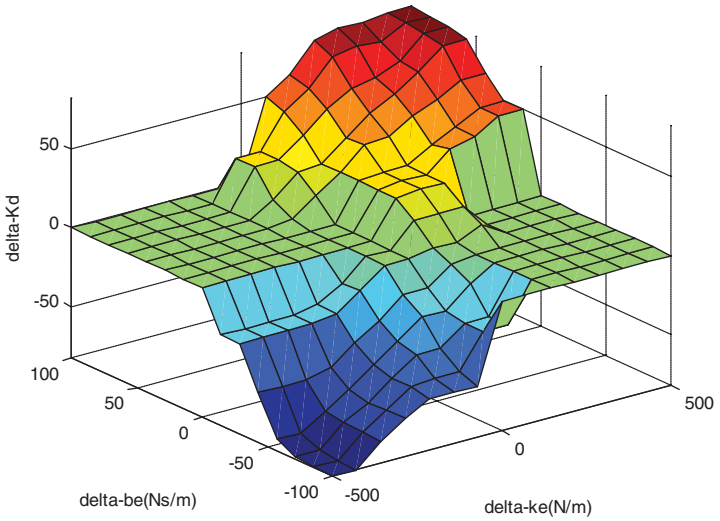
where B_d and K_d are the desired damping and stiffness, respectively. X_d and X are the desired and actual positions respectively, and $\dot{X}_d$ and $\dot{X}$ are the desired and actual velocities of the robot, respectively. F_d is the desired force between the robot and the impaired limb.

For the proposed fuzzy impedance force controller, the WAM generates an adaptive force correlated with the impaired limb's muscle strength recovery level. The desired impedance control parameters are real-time regulated according to the on-line estimated impaired limb's bio-damping and bio-stiffness. Figure 5 shows the block diagram of the fuzzy-based impedance force controller. In the fuzzy impedance regulator, the impaired limb's bio-impedance parameter changes ($\Delta\hat{b}_e$ and $\Delta\hat{k}_e$) and the desired impedance increments (ΔB_d and ΔK_d) are selected as input and output variables, respectively. Separate fuzzy logic regulators were designed for ΔB_d and ΔK_d. Figure 6(a) depicts the MFs for the input and output variables. If the changes of the impaired limb's bio-damping and bio-stiffness, $\Delta\hat{b}_e$ and $\Delta\hat{k}_e$, are positive (implying that the impaired limb's muscle was strengthened), then positive increments for ΔB_d and ΔK_d are added. On the contrary, if the changes of $\Delta\hat{b}_e$ and $\Delta\hat{k}_e$, are negative (small muscle strength was generated), then proportional negative increments for ΔB_d and ΔK_d should be supplied. As a typical description, Fig. 6(b) presents the control surface of the proposed fuzzy stiffness controller. In order to achieve accurate interaction force tracking, the desired force, f_d, generated from the proposed fuzzy impedance force controller and the actual force feedback, f_{active}, from the stroke subject, are incorporated into a PD force tracking regulator. The

https://doi.org/10.1017/S0263574713001264 Published online by Cambridge University Press



(a) Membership functions for input and output variables



(b) Control surface of fuzzy stiffness controller

Fig. 6. (Colour online) Description of membership functions for input and output variables in fuzzy force controller: (a) membership functions for input and output variables; (b) control surface of fuzzy stiffness controller.

following force tracking control law is thus obtained:

$$\tau_F = K_P(f_d - f_{\text{active}}) + K_D \frac{\mathrm{d}(f_d - f_{\text{active}})}{\mathrm{d}t}, \tag{12}$$

where

$$f_d = (B_d + \Delta B_d)(\dot{X}_d - \dot{X}) + (K_d + \Delta K_d)(X_d - X). \tag{13}$$

As mentioned before, gravity compensation should also be considered here. The gravity compensation coefficient, G_{scale}, may be set from the lower limit of 0.0 to the upper limit of 1.0, depending on the recovery condition of the impaired limb's muscle strength. The overall joint input torque τ can be reformulated as follows:

$$\tau = K_P(f_d - f_{\text{active}}) + K_D \frac{\mathrm{d}(f_d - f_{\text{active}})}{\mathrm{d}t} + M \cdot G_{\text{scale}} \cdot g. \tag{14}$$

https://doi.org/10.1017/S0263574713001264 Published online by Cambridge University Press

2.5. Safety

Ensuring safety of the stroke subjects is a very important issue when designing a robot-aided rehabilitation system. The WAM rehabilitation safety system consists of pendants and a safety board/module, which are used to monitor joint torque and velocity, communication between the computer and the Pucks^{TM}, voltage levels suitable to the WAM, and safety states, namely, E-STOP, IDLE, and ACTIVATED. The safety module will register a heartbeat fault and shut down the WAM manipulator in case the corresponding joint torque and velocity/voltage levels exceed the predefined limits or any motor controllers fail to issue communication. In addition, the robot can also be stopped by shutting down the power supply with an emergency button located near the stroke subject or the physical therapist.

3. Results

3.1. Position and torque control for passive training

Figure 7 shows the trapezoidal and sinusoidal trajectory tracking performances of the fuzzy and traditional PID position controllers with regard to a stroke subject sample in the vertical (J4, the 4th joint) elbow flexion/extension exercises. The impaired limb's flexion/extension limitations expressed in the WAM world frames were defined as –5.5 rad in flexion and –3.5 rad in extension. Conventional and initial fuzzy PID position controller gains, K_P, K_I, and K_D, were set as 600, 0.5, and 1.5, respectively. The safety peak joint velocity and the maximum motor torque for the four motors were set as 1.2 rad/s and 8191, respectively. It can be seen in Figs. 7(a) and 7(b) that when the stroke subject is guided by the WAM along the predefined trapezoidal and sinusoidal trajectories, the joint position control smoothness of the fuzzy-based PID position controller is obviously superior to the traditional PID controller, which can be found from the trajectory tracking error and joint velocity tracking. Further comparison with the results in sinusoidal and trapezoidal trajectories tracking shows that the former has smaller tracking error and better smoothness than the latter. This is because a new angle increment has been applied to the impaired limb in the trapezoidal trajectory and the patient's central nervous system needs sometime to accommodate itself to the new training task. As a comparison, trapezoidal trajectory tracking with two position controllers on a healthy subject is also presented in Fig. 7(c). It is obvious that the trajectory tracking error and joint velocity adjustment for the healthy subject are much smaller than the ones for the stroke subject. This is because cogwheel rigidity and uniform muscle tone characteristics for healthy and hemiparesis subjects existed.

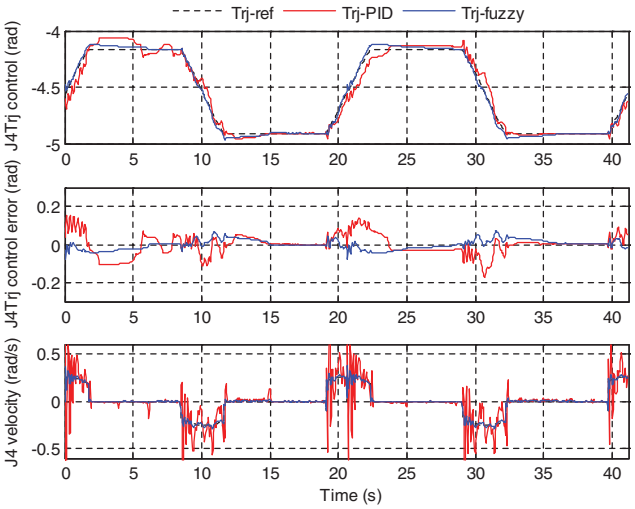
Similar performance advantages of fuzzy over the traditional PID position controller can be found from the horizontal (J3, the 3rd joint) trapezoidal and sinusoidal trajectories tracking, shown in Fig. 8. The limitations of the impaired limb's moveable ranges for horizontal shoulder flexion and extension were set as 0.8 rad and –0.8 rad, respectively. Traditional and initial fuzzy PID controller gains, K_P, K_I, and K_D, were set as 650, 2.5, and 10, respectively. Table III presents the means and standard deviations for the joint trajectory tracking error in each method.

Figure 9 shows joint torque control of two controllers corresponding to the position control shown in Figs. 7 and 8. The J4 and J3 torque control results for the stroke subject and the healthy subject samples further confirm that the fuzzy PID position controller outperforms the original PID controller with its smaller torque overshoot and vibration. It is also shown that the torque control performance of the two controllers for the stroke subject is inferior to the one for healthy subject. This may be attributed to the fact that the stroke subject is unable to control his/her impaired limb's muscle contraction freely.

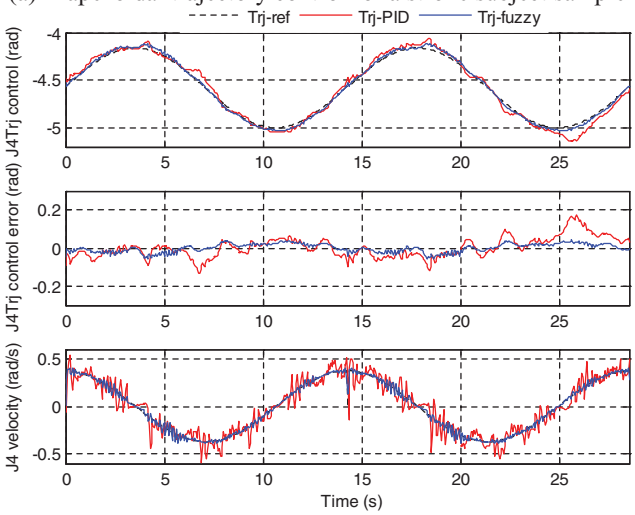
3.2. Parameter estimation and resistive force control for progressive resistance muscle strength training

Figure 10 presents the representative results of the impaired limb's bio-damping/bio-stiffness estimation and force regulation regarding fuzzy and traditional impedance force controllers in vertical resistance training. The parameters x_e, T, $\lambda_{\max}$,$\lambda_{\min}$, l, R, θ_0,P_0 of AFRLS were set as 0.576, 0.05, 0.9, 0.08, 5, 30, [0.000001; 0.000001], and [2500000, 2500000; 1500000, 1500000], respectively. For the conventional impedance controller, B_d and K_d were set as 2.5 and 35, respectively. Using

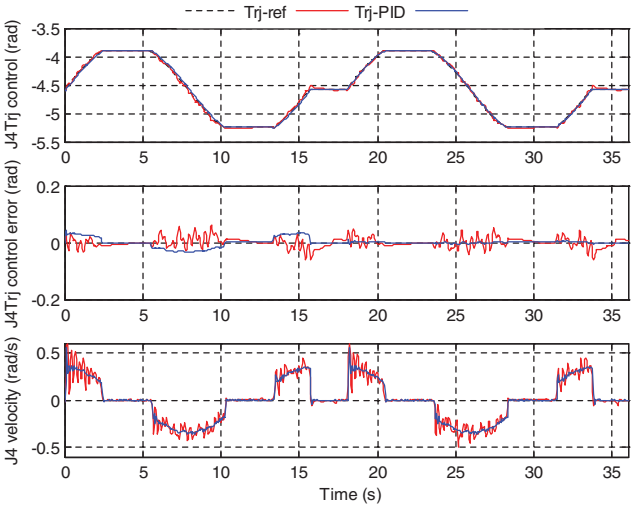
https://doi.org/10.1017/S0263574713001264 Published online by Cambridge University Press



(a) Trapezoidal trajectory control for a stroke subject sample



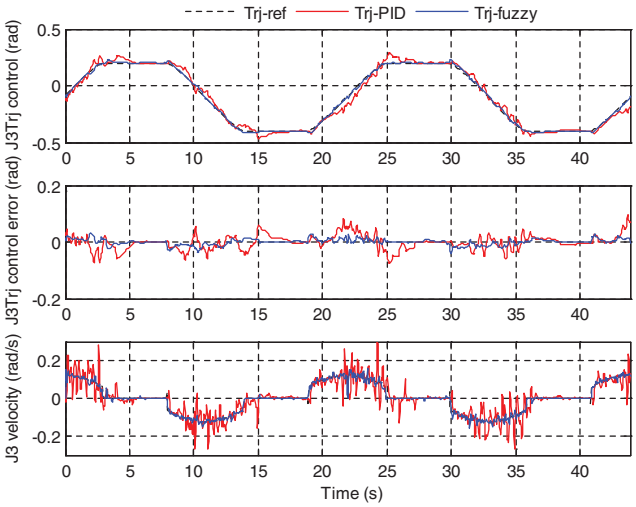
(b) Sinusoidal trajectory control for a stroke subjectsample



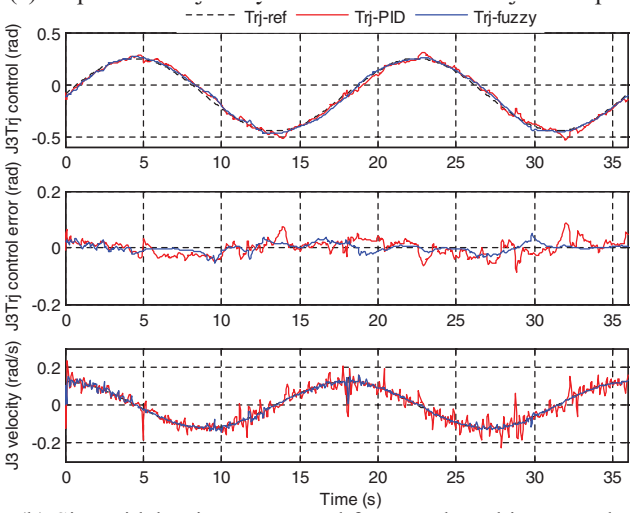
(c) Trapezoidal trajectory control for a healthy subject sample

Fig. 7. (Colour online) Representative results of trapezoidal and sinusoidal trajectory control in vertical elbow flexion/extension: (a) trapezoidal trajectory control for a stroke subject sample; (b) sinusoidal trajectory control for a stroke subject sample; and (c) trapezoidal trajectory control for a healthy subject sample.

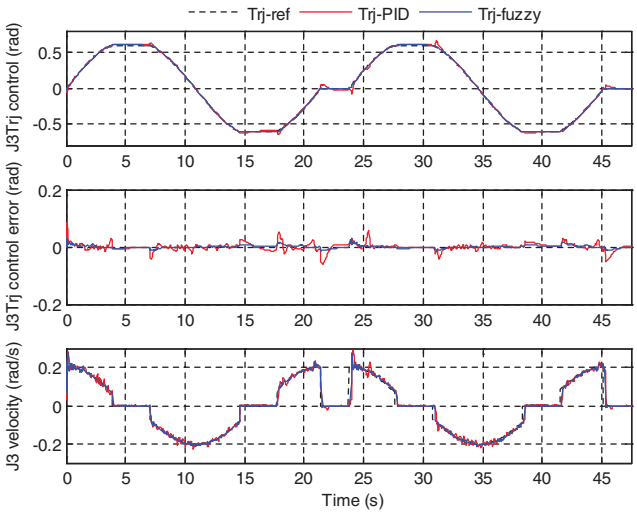
https://doi.org/10.1017/S0263574713001264 Published online by Cambridge University Press



(a) Trapezoidal trajectory control for a stroke subject sample



(b) Sinusoidal trajectory control for a stroke subject sample



(c) Trapezoidal trajectory control for a healthy subject sample

Fig. 8. (Colour online) Representative results of trapezoidal and sinusoidal trajectory control in horizontal shoulder flexion/extension: (a) trapezoidal trajectory control for a stroke subject sample; (b) sinusoidal trajectory control for a stroke subject sample; and (c) trapezoidal trajectory control for a healthy subject sample.

https://doi.org/10.1017/S0263574713001264 Published online by Cambridge University Press

Table III. A comparison of the means and standard deviations for joint trajectory tracking error in each method.

	Trapezoidal		Sinusoidal
	Stroke	Healthy	Stroke
Fuzzy_V	0.0092 ± 0.0043	0.00017 ± 0.0012	0.0054 ± 0.0036
Traditional_V	0.0560 ± 0.073	0.0064 ± 0.0085	0.057 ± 0.065
Fuzzy_H	0.0053 ± 0.0028	0.00013 ± 0.0013	0.0045 ± 0.0020
Traditional_H	0.051 ± 0.0531	0.0034 ± 0.0056	0.0472 ± 0.0531

Note: V = vertical elbow flexion/extension; H = horizontal shoulder flexion/extension.

the proposed fuzzy impedance regulator, B_d and K_d increments can vary from –50 to 50 and –100 to 100, respectively. The PD force tracking controller parameters were set as $K_P = 50$ and $K_D = 85$.

In Fig. 10(a)-a, the recruited stroke participant was asked to actively move the WAM along the predefined semi-sinusoidal trajectory and to perform the extension resistive exercises in the X^+OZ^- area. A 5 N initial resistive force was exerted and full gravity compensation for the WAM was made. It is observed that the impaired limb has moved the WAM away from the lower limit of the training trajectory quickly, and the estimated bio- damping and bio-stiffness parameters also show a substantial increase. This indicates that the stroke subject has sufficient muscle power to overcome the 5 N initial resistive force. It is also shown that once the increased damping and stiffness parameters go beyond the predefined thresholds for certain periods, the proposed fuzzy impedance controller is triggered and the generated desired resistive force will increase correspondingly. Then more energy will be consumed while doing the same exercises and this is beneficial to the impaired limb's muscle force training. The same conclusions can be drawn from the results in Fig. 10(a)-b, where the stroke participant was asked to perform flexion resistive exercises in the X^+OZ^+ area and a –5 N initial resistive force was exerted. Compared with the estimated bio-damping and bio-stiffness in Figs. 10(a) and 10(b), it is easy to see that the values of the former are clearly smaller than the ones of the latter (due to 9 N initial resistive force applied in the late resistance training).

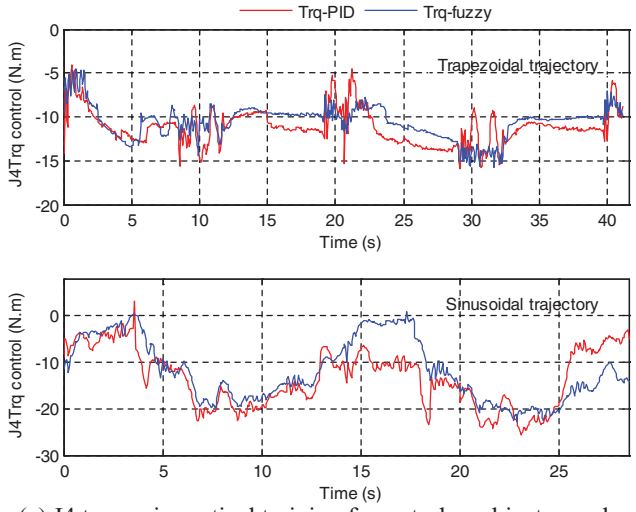
Figure 11 shows the estimation and force control results in horizontal resistance flexion/extension exercises, where the stroke subject was asked to perform flexion movement in the X^+OY^- area and extension in the X^+OY^+ area. 5 N and 9 N initial resistive forces were still exerted and the direction of the initial resistive force was altered to retain the resistance when the direction of movement was reversed. Comparing the profiles in Figs. 11(a)-a,c and 11(b)-a,c, the same conclusions as those in vertical resistive movements can be drawn, which include the estimated arm parameters and the desired resistive force values generated from two impedance controllers. In addition, as seen in Figs.11(a)-b and 11(b)-b, when the stroke subject exerted a certain muscle force to move the WAM close to the predefined trajectory, it is observed that the impaired limb's damping and stiffness converge to a fixed estimated value. This is because almost no force is generated from the two impedance controllers and only initial resistive force is applied to the impaired limb. It is further confirmed that nearly constant damping and stiffness parameters should be held when the patient generates invariable muscle force.

Table IV gives the maximum desired resistive force values generated from two impedance force controllers in vertical and horizontal progressive resistance muscle strength training. Obviously, the values generated from the fuzzy impedance controller are bigger than the ones from the traditional impedance controller. Unfortunately, force-tracking errors still exist in both vertical and horizontal flexion/extension resistive movements.

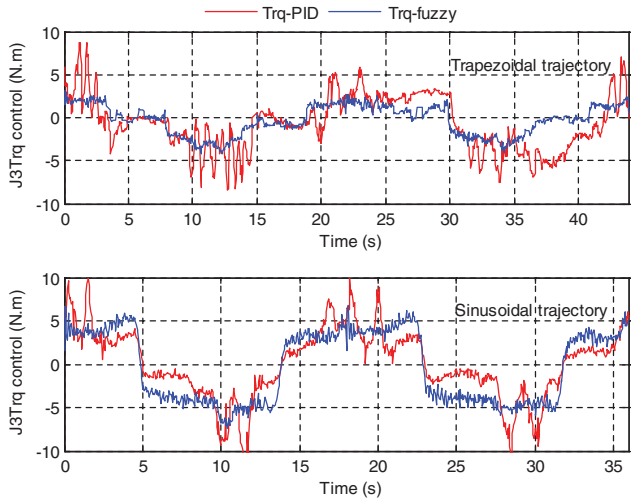
3.3. Therapy outcome evaluation and statistical analysis

The data was compared to determine the effectiveness of the robot assisted versus conventional therapy treatments. As mentioned in Section 2.3.3, PROM and MRF were selected as the primary outcome measures for the robot and conventional groups. Subjects in both groups were requested to perform five successful trials and the average test values were used as final evaluation results. The difference in each outcome measure from pre- to post-training was statistically analyzed with student's *t*-test methods using SPSS statistical software (Lead Technologies, Inc., Chicago, USA). Those *p*-values of 0.05 or less were considered as statistically significant. In the recruited 45 stroke

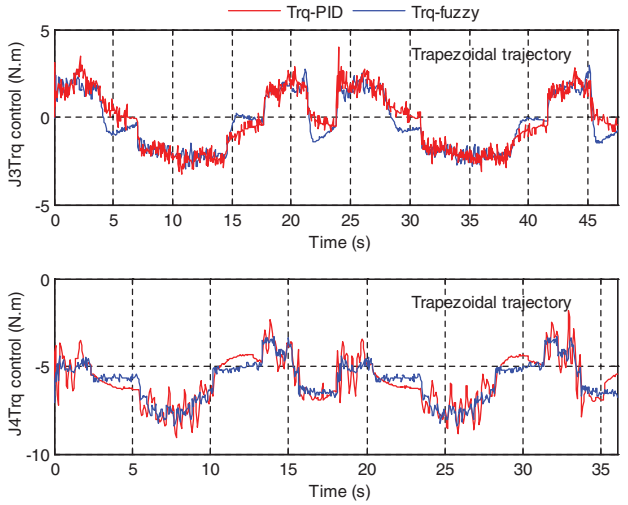
https://doi.org/10.1017/S0263574713001264 Published online by Cambridge University Press



(a) J4 torque in vertical training for a stroke subject sample



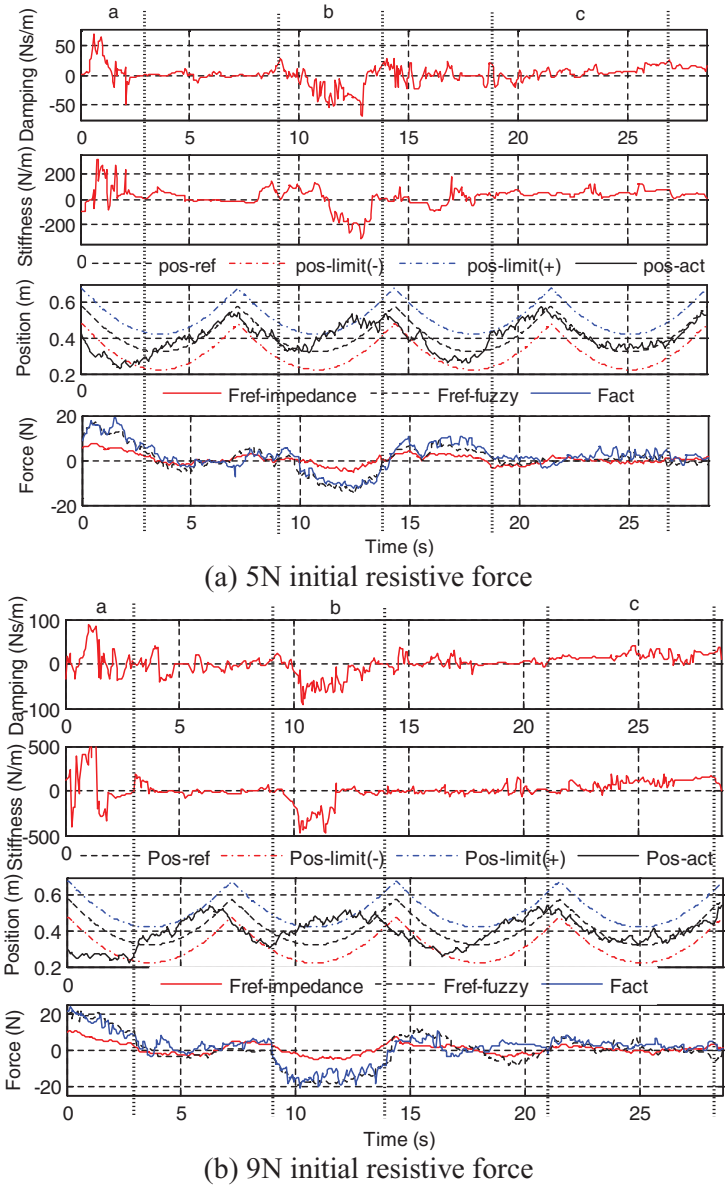
(b) J3 torque in horizontal training for a stroke subject sample



(c) J3 and J4 torque control for a healthy subject sample

Fig. 9. (Colour online) Representative results of joint torque control for vertical elbow and horizontal shoulder flexion/extension: (a) J4 torque in vertical training for a stroke subject sample; (b) J3 torque in horizontal training for a stroke subject sample; and (c) J3 and J4 torque control for a healthy subject sample.

https://doi.org/10.1017/S0263574713001264 Published online by Cambridge University Press



(a) 5N initial resistive force

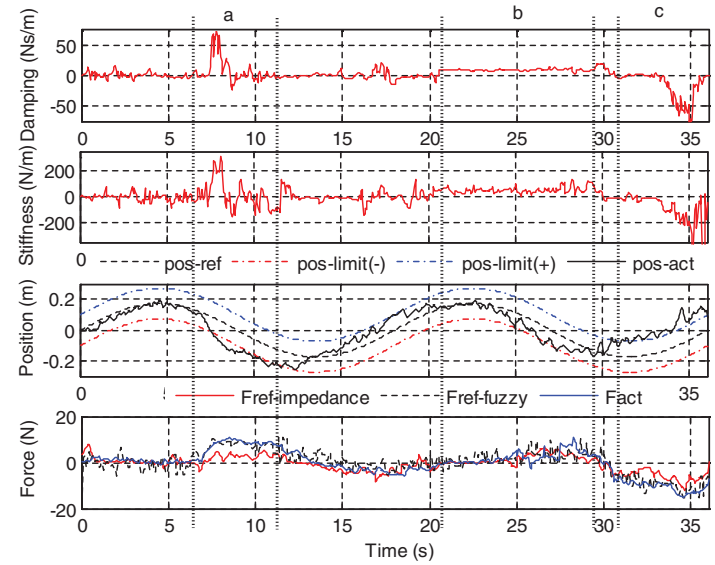
(b) 9N initial resistive force

Fig. 10. (Colour online) Representative results of arm parameter estimation and force regulation with different initial resistive forces in vertical flexion/extension progressive resistance muscle strength training: (a) 5 N initial resistive force and (b) 9 N initial resistive force.

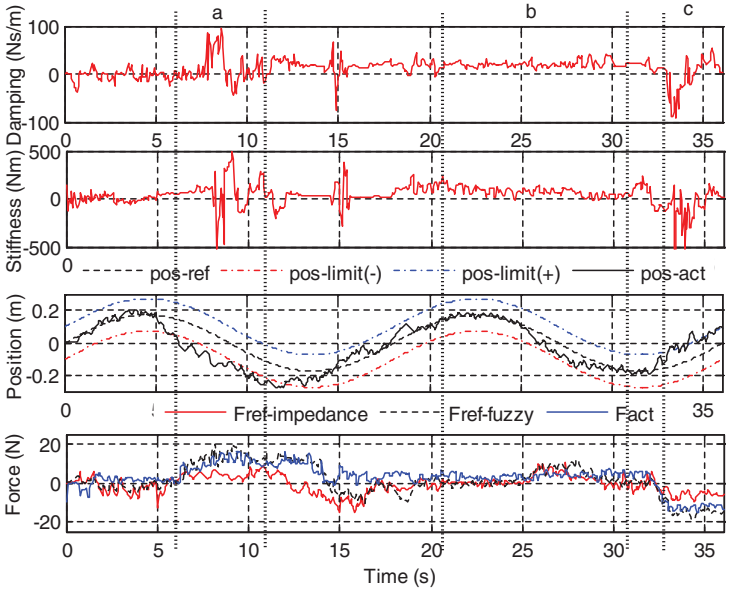
participants, five subjects (three in robot-aided therapy group and two in control group) were unable to complete the eight-week resistive training exercises after the passive and active training because of a recurrent stroke. Therefore, the therapy results of five subjects are only included in the PROM outcome analysis and not in the MRF measure. Table V shows the results of the therapy outcome evaluation and the statistical significance.

At the functional level, both groups performed well, with improvement in scores of two outcome measures, and showing clinical and statistical significance. Regarding the PROM and MRF outcome measures, individuals in the robotic therapy group, on an average, improved by (1.03 rad, $p = 0.000$) and (25.16 N, $p = 0.001$) in vertical flexion/extension, while (0.72 rad, $p = 0.000$) and (20.05 N, $p = 0.001$) in horizontal flexion/extension exercises. Under the conventional therapy, all saw certain improvements in the two outcome measures (PROM and MRF) of vertical and horizontal flexion/extension exercises: in PROM (0.92 rad, $p = 0.001$), (0.77 rad, $p = 0.001$); and in MRF (20.2 N, $p = 0.000$), (18.5 N, $p = 0.000$). Comparing the differences in the treatments of vertical

https://doi.org/10.1017/S0263574713001264 Published online by Cambridge University Press



(a) 5N initial resistive force



(b) 9N initial resistive force

Fig. 11. (Colour online) Representative results of arm parameter estimation and force regulation with a different initial resistive force in horizontal flexion/extension progressive resistance muscle strength training: (a) 5 N initial resistive force and (b) 9 N initial resistive force.

Table IV. Comparison of the maximum desired resistive force.

	Vertical			Horizontal	
	0–4.2 s	9.2–14.5 s	15.5–18.9 s	5.8–16.2 s	32.5–36 s
5 N initial resistive force					
Fuzzy	19.3145	–14.9244	10.7804	11.1116	–15.5794
Traditional	7.3581	–5.4165	3.9104	5.1883	–12.0339
9 N initial resistive force					
Fuzzy	23.6533	–21.2218	11.9779	19.6033	–19.3066
Traditional	15.1821	–6.8284	3.8406	15.1821	–9.3808

https://doi.org/10.1017/S0263574713001264 Published online by Cambridge University Press

Table V. Average improvements of two outcome measures under the experimental and conventional groups.

	PROM (rad)		MRF (N)	
	V	H	V	H
Experimental group				
Pre-training	0.85	0.77	10.16	10.37
Post-training	1.88	1.49	35.32	30.42
Mean change	1.03	0.72	25.16	20.05
Standard error change	0.013	0.003	1.113	0.561
p-value	0.000	0.000	0.001	0.001
Control group				
Pre-training	0.79	0.71	9.70	9.75
Post-training	1.71	1.48	29.90	28.25
Mean change	0.92	0.77	20.2	18.5
Standard error change	0.01	0.002	0.938	0.481
p-value	0.001	0.001	0.000	0.001
Therapy outcome comparison				
Difference in treatments	0.11	–0.05	4.96	1.55
Standard error difference	0.038	0.028	1.542	0.849
p-value	0.029	0.069	0.003	0.076

Note: V = vertical elbow flexion/extension; H = horizontal shoulder flexion/extension.

PROM (0.11, $p = 0.029$), horizontal PROM (–0.05, $p = 0.069$), vertical MRF (4.96, $p = 0.003$), and horizontal MRF (1.55, $p = 0.076$), it is clear that the improvements of the two outcome measures under robot-assisted therapy are greater than those under conventional therapy with the exception of the horizontal PROM measure. Moreover, significant differences in the vertical PROM and MRF assessments are revealed but not shown in the horizontal outcome measures. After consulting with the clinical therapist, it was determined that this may be attributed to the fact that the planned vertical flexion/extension training exercises are relatively compatible with the stroke patient's activities of daily living, while not so in the horizontal flexion/extension training. According to the planned horizontal exercises, the impaired limb's movement zone is constrained to the horizontal plane, and this does not coincide well with the clinical proprioceptive neuromuscular facilitation recovery exercise.

4. Discussions

Clinical experiments and quantitative assessments based on 24 stroke subjects were carried out on a Barrett WAM^{TM} manipulator using the proposed fuzzy position and impedance force therapy control algorithms. In the passive stretching exercises for vertical elbow flexion/extension and horizontal shoulder flexion/extension, fuzzy and conventional PID position control algorithms can both achieve the desired trapezoidal and sinusoidal trajectories, but the motion smoothness of the former is much better than the latter. Moreover, compared with the results for the healthy subject in our previous work,[16] stable and smooth motion control capabilities are still observed for the fuzzy position control algorithm, even in the presence of incorporating real-time biomechanical reflection from the stroke subject. This is beneficial for the stroke subject for improving PROM and achieving a normative joint movement pattern, especially in the case when unpredictable spasticity occurs.

In the progressive resistance muscle strength training, the most important advantage of the fuzzy impedance force therapy control strategy over the traditional impedance control method is that the proposed strategy will trigger the resistive force regulation between the WAM and the impaired limb when the stroke subject's bio-damping and bio-stiffness exceed predefined thresholds for some periods. The new algorithm fully encourages the stroke subject's active effort and self initiated movements. When the stroke subject's muscle is strengthened, the resistive force generated from the fuzzy impedance force controller is also augmented and the patient is further challenged. More

https://doi.org/10.1017/S0263574713001264 Published online by Cambridge University Press

energy will be consumed accomplishing the same task and this is beneficial to the impaired limb's muscle strength restoration.

5. Conclusions

In this paper, clinical experimental research on fuzzy adaptive robotic therapy control algorithms for robot-aided upper-limb rehabilitation are presented. Experimental results and therapy outcome assessments carried out on a Barrett WAM^{TM} manipulator verify that (1) in the passive recovery training, a fuzzy-based PID position controller can control the WAM robot stably and smoothly while stretching the impaired limb along the progressively increased training trajectories, even in the presence of incorporating real-time biomechanical reflection from the stroke subject; (2) in the progressive resistance muscle strength training, it is confirmed that the proposed fuzzy impedance force therapy controller outperforms the conventional impedance controller, since the former has the ability to generate adaptive resistive force correlated with the impaired limb's muscle force recovery level; and (3) robot-aided therapy alone, i.e., without additional physical therapy interventions tailored to the impaired limb, is as effective as standard physiotherapy treatment and even more effective for improving the joint range of motion and muscle strength.

Acknowledgements

The authors thank Dr. M. Kendal Ackerman, from the Department of Mechanical Engineering at Johns Hopkins University, for his assistance with the editing. This work is jointly supported by the National Natural Science Foundation of China (61305095, 61104216, and 61104206), the Natural Science Foundation for Colleges and Universities of Jiangsu Province of China (12KJB510015), and the Scientific Research Foundation of Nanjing University of Posts and Telecommunication (NY211020 and NY211067).

References

1. R. Riener, T. Nef and G. Colombo, "Robot-aided neurorehabilitation of the upper extremities," *Med. Biol. Eng. Comput*. **43**, 2–10 (2005).
2. L. M. Crespo and D. J. Reinkensmeyer, "Review of control strategies for robotic movement training after neurologic injury," *J. Neuro Eng. Rehabil.* **6**(20), 1–15 (2009).
3. H. P. H. Anh and K. K. Ahn, "Online tuning gain scheduling MIMO neural PID control of the 2-axes pneumatic artificial muscle (PAM) robot arm," *Expert Syst. Appl*. **37**, 6547–6560 (2010).
4. M. K. Chang, "An adaptive self-organizing fuzzy sliding mode controller for a 2-DOF rehabilitation robot actuated by pneumatic muscle actuators," *Control Eng. Pract.* **18**(1), 13–32 (2010).
5. D. Novak, M. Mihelj and R. Riener, "Psychophysiological measurements in a bio-cooperative feedback loop for upper extremity rehabilitation," *IEEE Trans. Neural Syst. Rehabil. Eng.* **19**(4), 400–410 (2011).
6. A. Frisolia, F. Salsedoa, M. Bergamascoa, B. Rossib and M. C. Carboncini, "A force-feedback exoskeleton for upper-limb rehabilitation in virtual reality," *Appl. Bionics Biomech.* **6**, 115–126 (2009).
7. J. F. Veneman, R. Kruidhof, E. E. Hekman, R. Ekkelenkamp, E. H. Van Asseldonk and H. Van der Kooij, "Design and evaluation of the LOPES exoskeleton robot for interactive gait rehabilitation," *IEEE Trans. Neural Syst. Rehabil. Eng*. **15**(3), 379–385 (2007).
8. K. Kiguchi and Y. Hayashi, "An EMG-based control for an upper-limb power-assist exoskeleton robot," *IEEE Trans. Syst. Man. Cybern. B Cybern.* **42**(4), 1064–1071 (2012).
9. K. Kiguchi, M. H. Rahman, M. Sasaki and K. Teramoto, "Development of a 3 DOF mobile exoskeleton robot for human upper-limb motion assist," *Robot. Auton. Syst.* **56**, 678–691 (2008).
10. G. Xu, A. Song and H. Li, "Control system design for an upper-limb rehabilitation robot," *Adv. Robot.* **25**(1), 229–251 (2011).
11. G. Xu, A. Song and H. Li, "Adaptive impedance control for upper-limb rehabilitation robot using evolutionary dynamic recurrent fuzzy neural network," *J. Intell. Robot. Syst.* **62**, 501–529 (2011).
12. S. M. Mizanoor Rahman and R. Ikeura, "A novel variable impedance compact compliant ankle robot for overground gait rehabilitation and assistance," *Procedia Eng.* **41**, 522–531 (2012).
13. R. Jiménez-Fabián and O. Verlinden, "Review of control algorithms for robotic ankle systems in lower-limb orthoses, prostheses, and exoskeletons," *Med. Eng. Phys.* **34**(4), 397–408 (2012).
14. A. M. Hughes, C. T. Freeman, J. H. Burridge, P. H. Chappell, P. L. Lewin and E. Rogers, "Shoulder and elbow muscle activity during fully supported trajectory tracking in people who have had a stroke," *J. Electro. Kines.* **20**(3), 465–476 (2010).
15. G. Xu, A. Song, L. Pan, H. Li, Z. Liang, S. Zhu, B. Xu and J. Li, "Adaptive hierarchical control for muscle strength training of stroke survivors in robot-aided upper-limb rehabilitation," *Int. J. Adv. Robot. Syst.* **9**, 1–12 (2012).

https://doi.org/10.1017/S0263574713001264 Published online by Cambridge University Press

16. A. Song, J. Wu, G. Qin and W. Huang, "A novel self-decoupled four degree-of-freedom wrist force/torque sensor," *Measurement* **40**, 883–891 (2007).
17. J. H. Ryu, D. S. Kwon and B. Hannaford, "Stable teleoperation with time-domain passivity control," *IEEE Trans. Robot. Autom.* **20**(2), 365–373 (2004).
18. A. Song, L. Pan, G. Xu and H. Li, "Impedance Identification and Adaptive Control of Rehabilitation Robot for Upper Limb Passive Training," *Proceedings of the 7th International Conference on Intelligent Systems and Knowledge Engineering*, Beijing, China (Dec. 15–17, 2012).
19. T. Noritsugu and T. Tanaka, "Application of rubber artificial muscle manipulator as a rehabilitation robot," *IEEE Trans. Mechanics* **2**(4), 259–267 (1997).
20. L. Q. Zhang, S. G. Chung, Z. Bai, D. Xu, E. M. van Rey, M. W. Rogers, M. E. Johnson and E. J. Roth, "Intelligent stretching of ankle joints with contracture/spasticity," *IEEE Trans. Neural Syst. Rehabil. Eng*. **10**, 149–157 (2002).
21. V. Mallapragada, D. Erol and N. Sarkar, "A new method of force control for unknown environments," *Int. J. Adv. Robot. Syst*. **4**(3), 313–322 (2007).

https://doi.org/10.1017/S0263574713001264 Published online by Cambridge University Press